Neurobiology of Disease xxx (2013) xxx–xxx

Contents lists available at SciVerse ScienceDirect

Neurobiology of Disease

journal homepage: www.elsevier.com/locate/ynbdi

Altered Purkinje cell miRNA expression and SCA1 pathogenesis

Edgardcxo Rodriguez-Lebron [a], Gumei Liu [a,d], Megan Keiser [d], Mark A. Belhke [e], Beverly L. Davidson [a,b,c,d,*]

[a] Department of Internal Medicine, University of Iowa, Iowa City, IA 52242, USA
[b] Department of Neurology, University of Iowa, Iowa City, IA 52242, USA
[c] Department of Molecular Physiology & Biophysics, University of Iowa, Iowa City, IA 52242, USA
[d] Department of Neuroscience, University of Iowa, Iowa City, IA 52242, USA
[e] Integrated DNA Technologies Inc., Coralville, IA 52241, USA

ARTICLE INFO

Article history:
Received 6 August 2012
Revised 7 January 2013
Accepted 17 January 2013
Available online xxxx

Keywords:
Spinocerebellar ataxia
Polyglutamine
Ataxin-1
miRNA
miR-150
Vegfa
RNA interference
AAV
Cerebellum
Neurodegeneration

ABSTRACT

Spinocerebellar ataxia type 1 (SCA1) is a dominantly inherited neurodegenerative disorder caused by polyglutamine repeat expansions in Ataxin-1. Recent evidence supports a role for microRNAs (miRNAs) deregulation in SCA1 pathogenesis. However, the extent to which miRNAs may modulate the onset, progression or severity of SCA1 remains largely unknown. In this study, we used a mouse model of SCA1 to determine if miRNAs are misregulated in pre- and post-symptomatic SCA1 cerebellum. We found a significant alteration in the steady-state levels of numerous miRNAs prior to and following phenotypic onset. In addition, we provide evidence that increased miR-150 levels in SCA1 Purkinje neurons may modulate disease pathogenesis by targeting the expression of *Rgs8* and *Vegfa*.

Published by Elsevier Inc.

Introduction

Spinocerebellar ataxia type 1 (SCA1) is a member of the polyglutamine (polyQ) family of diseases, a group of dominantly inherited neurodegenerative disorders caused by the expansion of translated CAG trinucleotide repeats (Orr, 2012; Zoghbi and Orr, 2009). In SCA1, the expanded polyQ tract resides near the *N*-terminus of the Ataxin-1 (Atxn1) protein (Banfi et al., 1994). Although mutant Atxn1 is expressed throughout the brain, SCA1 is primarily characterized by the loss of cerebellar Purkinje cells and degeneration of the spinocerebellar tracts (Durr, 2010; Seidel et al., 2012). While the exact molecular mechanisms underlying this selective neurodegeneration remain largely unknown, it has been suggested that the deregulation of gene expression programs may, in part, explain this cell and region-specific vulnerability (Crespo-Barreto et al., 2010; Matilla-Duenas et al., 2010; Serra et al., 2004).

Altered neuronal transcriptional activity is an early and persistent pathomolecular feature of most polyglutamine diseases (Orr and Zoghbi, 2007; Takahashi et al., 2010; Verbeek and van de Warrenburg, 2011). Changes in the steady-state levels of numerous mRNA transcripts are seen in the cerebella of SCA1 patients and mouse models of the disease (Crespo-Barreto et al., 2010; Cvetanovic et al., 2011; Fernandez-Funez et al., 2000; Lin et al., 2000; Serra et al., 2004). Since wild-type Atxn1 functions within a transcriptional repressor complex that includes the DNA binding protein Capicua (Lam et al., 2006), transcriptional deregulation in SCA1 is thought to result from both a partial loss of Atxn1 function and a gain of toxic function in mutant Atxn1 (Lim et al., 2008; Orr, 2012). In fact, SCA1 mouse models have reduced the levels of the Atxn1-Capicua transcriptional repressor complex and a corresponding increase in the levels of some Atxn1-Capicua-regulated mRNAs (Crespo-Barreto et al., 2010). However, the steady-state levels of numerous other mRNAs not directly regulated by the Atxn1-Capicua complex are also altered early in the pathogenesis of SCA1. This suggests that other cellular pathways may play key roles in the pathogenesis of SCA1.

MicroRNAs (miRNAs) are small non-coding RNAs employed to post-transcriptionally regulate the steady-state levels of mRNA transcripts in the cell (Kim et al., 2009). Mounting evidence supports a role for microRNAs in the pathogenesis of SCA1. First, changes in steady-state levels of several miRNAs are observed in human SCA1 brains (Persengiev et al., 2011). Second, disrupting miRNA biogenesis in Purkinje neurons leads to ataxia and cerebellar degeneration reminiscent of SCA1 and other dominantly inherited ataxias (Schaefer et

* Corresponding author at: University of Iowa, Department of Internal Medicine, Room 200, Eckstein Medical Research Building, Iowa City, IA 52242, USA. Fax: +1 319 353 5572.
E-mail address: beverly-davidson@uiowa.edu (B.L. Davidson).
Available online on ScienceDirect (www.sciencedirect.com).

0969-9961/$ – see front matter Published by Elsevier Inc.
http://dx.doi.org/10.1016/j.nbd.2013.01.019

al., 2007). Finally, the Atxn1 mRNA itself is posttranscriptionally regulated by several miRNAs, some of which display increased activity in the human SCA1 brain (Lee et al., 2008; Persengiev et al., 2011). Nevertheless, the extent to which miRNA deregulation in SCA1 may drive early events in the pathogenesis of the disease remains largely unknown.

Here, we profiled global miRNA expression in the cerebellum of pre- and post-symptomatic SCA1 transgenic mice. As was reported for human SCA1 brains, we find significant changes in the expression of several miRNAs. We also provide evidence that a number of miRNAs display altered steady-state levels prior to the onset of measurable phenotypes. In addition, we establish a connection between increased miR-150 levels and the loss of *Vegfa* mRNA in SCA1 mouse brain. These results shed new light into the role that miRNAs play in the pathogenesis of SCA1 and provide new opportunities for the development of disease biomarkers and therapies.

Materials and methods

Animals

The SCA1 BO5 transgenic line used in this study was maintained in an FVB background. The mouse colony was bred and maintained at the University of Iowa animal vivarium. Mice were exposed to a 12-hour light-dark cycle and had access to food and water ad libitum. Transgenic and littermate control mice were genetically identified using established PCR-based protocols. All experiments involving animals were approved by Animal Care and Use Committee at the University of Iowa.

RNA collection, microRNA array and quantitative PCR

Cerebella were collected from wild-type and age matched SCA1 mice at 4 and 12 weeks of age (n = 4, per group) using TRIzol (Invitrogen) according to the manufacturer instructions. MiRNA expression profiles were obtained using miRCURY LNA™ all species microRNA arrays, miRBase version 9.2 (Exiqon, Vedbaek, Denmark). Individual miRNAs were analyzed by quantitative PCR (Q-PCR) using a high-capacity cDNA archive kit and TaqMan® MiRNA Assays (both from ABI). Gene specific Q-PCR was performed as above using random hexamer primers and TaqMan® Gene-Specific Expression Assays on an ABI-7900 instrument (ABI).

In situ hybridization

MicroRNA in situ hybridization was performed using short digoxigenin-labeled DNA–LNA probes (Exiqon). Briefly, fresh frozen 12 μm sections were post-fixed in 4% paraformaldehyde and washed in PBS. Prior to hybridization, sections were acetylated by washing in 1.32% triethanolamine solution followed by acetic anhydride treatment. Sections were prehybridized for 2 h at 55 °C, then hybridized at 55 °C overnight (prehybridization and hybridization buffer were purchased from Ambion, mRNA locator kit). After hybridization, sections were washed in 2× SSC at 55 °C three times for 90 min, and then briefly rinsed in PBST (0.1% Tween 20 in PBS). Sections were blocked with 2% sheep serum in PBST at room temperature for 1 h, and incubated in alkaline phosphatase (AP) conjugated anti-digoxigenin antibody (Roche) at 1:1000 at 4 °C overnight. Color reaction was carried in AP buffer (100 mM Tris–HCl, 50 mM MgCl2, 100 mM NaCl, 0.1% Tween-20, pH 9.5) containing NBT/BCIP (50× stock solution, Roche).

Anti-Vegfa immunohistochemistry

Mice were transcardially perfused with saline solution followed by 4% paraformaldehyde (PFA, pH 7.4). Dissected brains were fixed overnight in 4% PFA and immersed in cryoprotectant (30% sucrose/0.1 M PBS) for 48-h at 4 °C. Sagittal cerebellar sections (30 μm) were obtained on a sliding microtome and stored frozen in a 30% sucrose–30% ethylene glycol/0.1 M PBS solution. All sections were washed in 0.1 M PBS, overnight, prior to histological processing. The anti-Vegfa antibody stain was performed following manufacturer's recommendations (Abcam, ab39250). Briefly, sections were incubated for 20 min in a 10 mM sodium citrate buffer (pH 6.0), 0.05% Tween 20 solution preheated to and maintained at 100 °C. Following the antigen retrieval step, sections were blocked using 0.1 M PBS with 0.05% Tween 20 and 5% normal goat serum. Sections were next incubated for 3 days at 4 °C with anti-Vegfa antibody (1:100) diluted in blocking solution. Finally, an Alexa Fluor®488-conjugated goat anti-rabbit secondary antibody was used at a 1:500 dilution. Images were captured using a Leica DM RBE fluorescent stereoscope.

N2A cell culture and transfections

Mouse Neuro2a cells were maintained in DMEM/F12 mix supplemented with 10% fetal bovine serum, L-glutamine (5 mM) and non-essential amino acids (0.1 mM). A *MirVana*™ miR-150 miRNA mimic and a *MirVana*™ miRNA control mimic were purchased from Applied Biosystems (Life Technologies, Carlsbad, CA). Transfection of the double-stranded miRNA mimics into Neuro2a cells was performed using RNAimax reagent (Life Technologies) following the manufacturer's recommendations. Total RNA or protein lysates were obtained as previously described.

The first 1.7 kb of the 3′ untranslated region of mouse Vegfa was amplified using conventional RT-PCR and the following primers: 5′-CCATAGATGTGACAAGCCAAGGC-3′ and 5′-CTGCTCTAGAGACAAAGACGTG-3′. To generate the mutant Vegfa-3′UTR the conserved miR-150 binding site (5′-TGCTGTGGACTTGTGTTGGGAGG-3′) was disrupted by deleting the underlined 12-nucleotide sequence using a previously described site-directed mutagenesis approach (Tsou et al., 2011). The resulting Vegfa-3′UTR sequences were cloned into the XhoI–NotI sites of the psiCHECK-2™ vector system (Promega, Fitchburg, WI). *Renilla* luciferase activity was measured following the manufacturer's recommendations (Promega) and normalized using the intraplasmid *firefly* luciferase normalization reporter.

Western blot analyses

Vegfa protein expression was detected in western blots using a rabbit polyclonal antibody (ab39250, 1:500 dilution; Abcam, Cambridge, UK). Tubulin levels (anti-α-tubulin, 1:10,000; Sigma, St Louis, MO) were analyzed and used to normalize the levels of Vegfa in western blots. Following 48-h of primary antibody incubation at 4 °C, membranes were washed and incubated with peroxidase-conjugated with either anti-rabbit or anti-mouse secondary antibodies (1:20,000 dilution; Jackson Immuno Research Laboratories, West Grove, PA). The signal was obtained using the ECL-plus reagent (*Western Lighting*, PerkinElmer, Waltham, MA) as previously described (Tsou et al., 2011). Quantification of band intensities was performed using the Quantity One Software analysis tool. We quantified Vegfa expression in three independent experiments by normalizing the Vegfa signal to the Tubulin signal and calculating the mean expression level in experimental groups (miR-150 mimic treatment) relative to the control groups (control miRNA mimic treatment).

AAV RNAi vectors

Artificial miRNAs targeting human ATXN1 or a control sequence were designed and cloned into shuttle recombinant adeno-associated viral vectors (rAAV) as previously described (Boudreau et al., 2009, 2011). High-titer rAAV virus used in this study was produced at the University of Iowa Gene Transfer Vector Core (Iowa City, IA) following previously described methods.

Please cite this article as: Rodriguez-Lebron, E., et al., Altered Purkinje cell miRNA expression and SCA1 pathogenesis, Neurobiol. Dis. (2013), http://dx.doi.org/10.1016/j.nbd.2013.01.019

Mouse cerebellar injections

AAV–RNAi vectors were delivered into the mouse deep cerebellar nuclei as previously described (Boudreau et al., 2009; Xia et al., 2004). Briefly, adult SCA1 transgenic mice (5–10 weeks of age) were anesthetized and immobilized on a stereotaxic frame. A Hamilton syringe fitted with a 33-gage needle was positioned at −6.0 mm anteroposterior, ±2.0 mm lateral, −2.2 mm dorso-ventral from the empirically determined *bregma* zero coordinate. A total of 4 μl of 1×10^{12} vg/ml of virus was infused bilaterally at a rate of 0.20 μl/min.

Statistical analysis

For microRNA microarray, data was normalized and differential gene expression was assessed using *t*-test. Genes were selected as differentially expressed if the lower bound of fold change was greater than 1.2-fold. Next, two-sample *t*-test statistics and their associated *P* values were computed for each probe set on transformed data after computing the base-two logarithm. To account for multiple testing, the *P* value was modeled as a β-uniform mixture. Genes were selected as differentially expressed by choosing a *P*-value cutoff that ensured that (False Discovery Rate) FDR was <5%. Luciferase data were analyzed for statistical significance using two-tailed Student's *t*-test (GraphPad Prism InStat, version 3). Statistical significance is reported for $P<0.05$ (*) and $P<0.01$ (**).

Results

Differential expression of microRNAs in the cerebellum of SCA1 transgenic mice

The miRCURY LNA™ microarray platform was used to profile global miRNA expression in the BO5 SCA1 transgenic mouse cerebellum. BO5 SCA1 transgenic mice (SCA1 transgenic) express mutant human Atxn1 with 82 polyQ repeats under the control of the Purkinje cell-specific *Pcp2* promoter (Burright et al., 1995). For this analysis, total cerebellar RNA was extracted from SCA1 transgenic and age-matched littermate control mice at 4 and 12 weeks of age (n = 3 per group/time point). These times represent pre- and post-symptomatic stages of pathogenesis in BO5 SCA1 transgenic mice. Moderate but statistically significant changes in expression were detected in a number of miRNAs in the SCA1 transgenic cerebellum compared to control mice at both 4- and 12-week time points (Table 1). Moderate changes were not surprising given the Purkinje cell-specific expression of mutant Atxn1 in the BO5 line. A total of 34 miRNAs displayed increased steady-state levels in the SCA1 transgenic mouse cerebellum. Among these, 14 miRNAs had significantly increased steady-state levels at both time points, 15 at the 4-week time point only and 5 at the post-symptomatic 12-week time point. Conversely, a total of 12 miRNAs showed a significant reduction in steady-state levels at either both time points (1 of 12), at the pre-symptomatic stage (4 of 12) or at the post-symptomatic stage (7 of 12).

Overall, there was a strong bias towards increased miRNA expression in SCA1 cerebella when compared to littermate controls (34 out of 46 differentially expressed miRNAs). We chose to validate, using quantitative PCR, the expression of a subset of miRNAs with increased steady-state levels at the 4-week (miR-150 and miR-335), 12-week (miR-23a) or at both the 4- and the 12-week time points (miR-24 and miR-143). Although there was disagreement in the magnitude of the fold change between the array and qPCR analyses, increased levels of miR-24 (1.37 fold), miR-150 (1.67 fold) and miR-335 (1.43 fold) were replicated in additional cerebellar samples from 12-week old SCA1 mice (Fig. 1A). The fact that modest but significant changes in miR-150 and miR-335 levels were detected at 12-weeks of age using miRNA qPCR assays, and not the array platform, is not surprising given the increased sensitivity and reproducibility of the former.

Table 1
Differentially expressed miRNAs in SCA1 mouse cerebella.

Expression	MicroRNA[a]	4 weeks		12 weeks	
		Fold change[b]	*P* value	Fold change[b]	*P* value
Increased	mmu-miR-22	1.587	0.00323	1.415	0.0425
	mmu-miR-125b	1.563	0.02370	1.543	0.0200
	mmu-miR-194	1.503	0.04094	1.211	0.0377
	mmu-miR-24	1.481	0.00646	1.424	0.0175
	mmu-miR-30c	1.463	0.03663	1.393	0.0125
	mmu-miR-16	1.449	0.01508	1.463	0.0137
	mmu-miR-191	1.426	0.01293	1.259	0.0400
	mmu-miR-143	1.420	0.00862	1.548	0.0112
	mmu-miR-376b	1.409	0.01831	1.304	0.0212
	mmu-miR-376a	1.350	0.01724	1.367	0.0225
	mmu-miR-26a	1.343	0.05004	1.956	0.0012
	mmu-miR-218	1.325	0.02909	1.203	0.0440
	mmu-miR-195	1.272	0.04849	1.662	0.0087
	mmu-miR-361	1.221	0.04525	1.253	0.0462
	mmu-miR-150	1.617	0.00431	–	–
	mmu-miR-100	1.521	0.01616	–	–
	mmu-miR-7	1.519	0.03017	–	–
	mmu-miR-146b	1.477	0.00538	–	–
	mmu-miR-335	1.416	0.03340	–	–
	mmu-miR-26b	1.414	0.01400	–	–
	mmu-miR-96	1.382	0.00754	–	–
	mmu-miR-379	1.377	0.01185	–	–
	mmu-miR-9*	1.352	0.02047	–	–
	mmu-miR-30b	1.329	0.03987	–	–
	mmu-miR-126-3p	1.320	0.03771	–	–
	mmu-miR-128b	1.287	0.04418	–	–
	mmu-miR-9	1.260	0.04202	–	–
	mmu-miR-31	1.259	0.03448	–	–
	mmu-miR-30d	1.230	0.04956	–	–
	mmu-miR-23a	–	–	1.393	0.0187
	mmu-miR-27a	–	–	1.309	0.0300
	mmu-miR-350	–	–	1.303	0.0412
	mmu-miR-129-3p	–	–	1.265	0.0375
	mmu-miR-99a	–	–	1.510	0.0050
Decreased	mmu-miR-381	0.617	0.03879	0.682	0.0100
	mmu-miR-203	0.796	0.05172	–	–
	mmu-miR-34c	0.710	0.02586	–	–
	mmu-miR-489	0.623	0.01939	–	–
	mmu-miR-224	0.465	0.00215	–	–
	mmu-miR-484	–	–	0.8089	0.0258
	mmu-miR-329	–	–	0.8073	0.0090
	mmu-miR-133b	–	–	0.7969	0.0612
	mmu-miR-423	–	–	0.7611	0.0437
	mmu-miR-138	–	–	0.7244	0.0362
	mmu-miR-487b	–	–	0.6993	0.0150
	mmu-miR-206	–	–	0.6918	0.0287

[a] Only microRNA probes with >1.2 fold change on miRCURY™ microarray are included.
[b] Fold change is shown relative to age matched healthy control littermates. Only fold changes with statistical significance ($P<0.05$) are shown.

To understand whether these changes were due to primary or secondary effects of expressing mutant Atxn1, we assessed whether changes in miRNA steady-state levels were proximal or distal to the onset of transgenic mutant Atxn1 expression in SCA1 transgenic mice. For this, total cerebellar RNA from 6-day old and 18-day old SCA1 transgenic and littermate controls was analyzed. At postnatal day 6, levels of transgenic mutant Atxn1 are barely detectable while at postnatal day 18 they have reached 50% of adult levels (data not shown). As shown in Fig. 1B, when compared to littermate controls (white bars), miR-150 and miR-335 levels were significantly higher (1.28 and 1.54 fold respectively, pattern bars) in 18-day old but not in 6-day old SCA1 cerebella (black bars). Together, these data indicate that the expression of a number of cerebellar miRNAs is affected prior to phenotypic onset, implicating miRNA deregulation as a possible driving force in the early pathogenesis of SCA1 transgenic mice.

In SCA1 transgenic mice, the expression of mutant Atxn1 is restricted to cerebellar Purkinje cells. Thus, we investigated if the changes in miR-150 expression also occurred selectively in this cell

Please cite this article as: Rodriguez-Lebron, E., et al., Altered Purkinje cell miRNA expression and SCA1 pathogenesis, Neurobiol. Dis. (2013), http://dx.doi.org/10.1016/j.nbd.2013.01.019

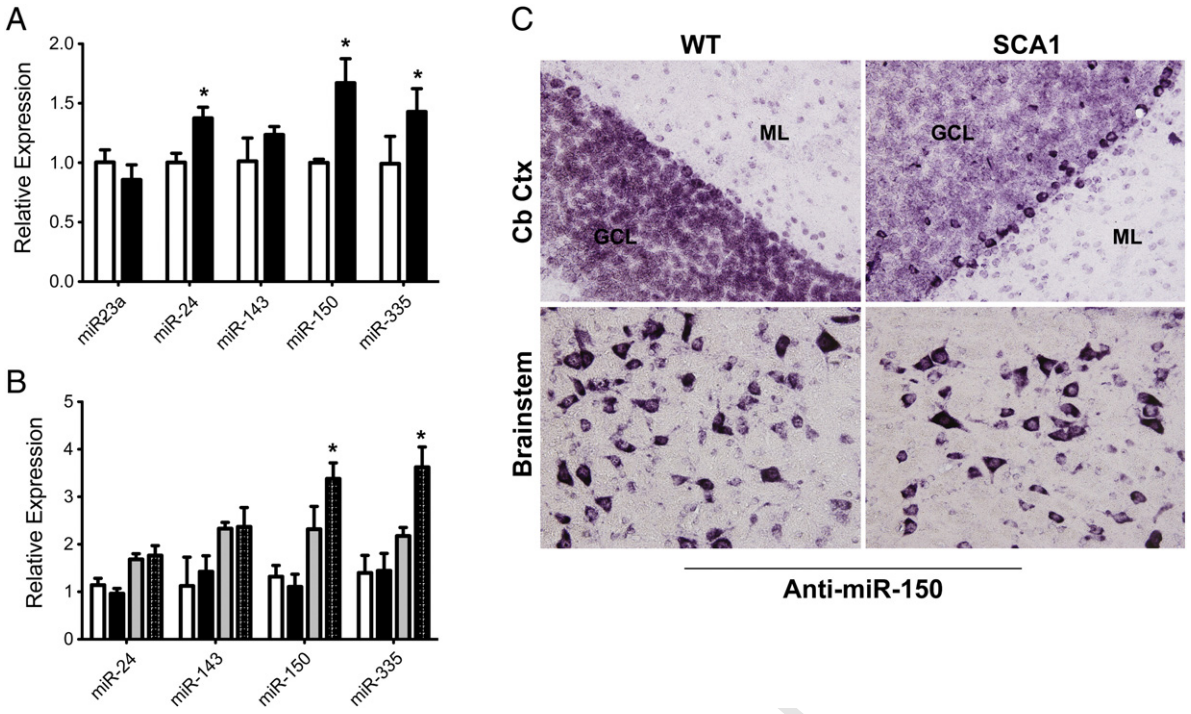

Fig. 1. Upregulation of miRNA expression in SCA1 cerebellum. A) Quantitative PCR analysis of miR-23a, miR-24, miR-143, miR-150 and miR-335 expression in adult SCA1 transgenic mouse cerebellum (black bars) compared to littermate controls (white bars). B) Quantitative PCR analysis of miR-24, miR-143, miR-150 and miR-335 expression in the cerebellum of 6-day old SCA1 transgenic (black bars) compared to 6-day old littermate controls (white bar) or in the cerebellum of 18-day old SCA1 transgenic (black patterned bars) compared to 18-day old littermate controls (gray bars). C) In situ hybridization using an anti-miR-150 probe. Increased probe signal was detected in the Purkinje cell layer of coronal cerebellar sections obtained from adult SCA1 transgenic mice (SCA1) compared to littermate controls (WT). There was also a measurable decrease in signal intensity in the SCA1 transgenic granule cell layer (GCL) when compared to controls. In contrast, the anti-miR-150 signal was similar in the cerebellar molecular layer (ML) and in the brainstem of SCA1 transgenic and littermate control mice. Error bars represent ± std. dev. * = $P<0.05$, student's *t*-test.

population. In situ hybridization analysis revealed a selective increase in the levels of miR-150 in SCA1 transgenic cerebellar Purkinje neurons (Fig. 1C, top right panel) when compared to wild-type Purkinje neurons (top left panel). This increase in miR-150 expression along the Purkinje cell layer was not observed in the granule cell layers. Instead, miR-150 expression was slightly decreased in SCA1 transgenic granule cells when compared to those in wild-type mice. miR-150 expression in brain stem-containing sections were similar between SCA1 transgenic and control littermates (Fig. 1C, bottom panels). These findings are consistent with a Purkinje cell specific pathogenic process involving the misregulation of miR-150 expression. Moreover, the slight decrease in miR-150 levels in granule cells hints that miRNA misregulation may underlie some non-cell-autonomous degeneration. In fact, a previous study suggested that cross talk between cerebellar Purkinje and granule cells might play a role in the SCA1 disease process (Gatchel et al., 2008).

MiR-150 targets the 3′UTR of Rgs8 and Vegfa

We hypothesized that increased miR-150 levels should be functionally manifested by a reduction in the levels of its target mRNAs. To gain insight into how increased miR-150 activity in Purkinje cells may modulate SCA1 pathogenesis we compiled a list of mRNAs reported to have reduced steady-state levels in SCA1 transgenic mice (Cvetanovic et al., 2011; Lin et al., 2000; Serra et al., 2004) and intersected it with a list containing the top predicted miR-150 mRNA targets (*TargetScan* Friedman et al., 2009; Grimson et al., 2007; Lewis et al., 2005). Our analysis identified two transcripts, *Rgs8* and *Vegfa*, which are predicted to be targets of miR-150 and appear to be altered in SCA1 (Fig. 2A) (Cvetanovic et al., 2011; Serra et al., 2004). Confirming previous findings (Cvetanovic et al., 2011), quantitative PCR analysis showed a significant but modest reduction in the levels of *Vegfa* and *Rgs8* mRNA (0.71 and 0.77 fold difference) in 12-week old SCA1 cerebella (Fig. 2B). To further validate our findings we analyze the expression of *Calbindin-1* mRNA, a well-established marker of SCA1 pathogenesis, and the expression of *Atxn3* mRNA, a control transcript anticipated to remain unchanged between transgenic and control mice. Importantly, both transcripts lack miR-150 binding sites in their 3′ untranslated regions and thus serve as valid controls. As expected, we detected a loss in *Calbindin-1* mRNA (0.34 fold difference) but not in *Atxn3* mRNA in 12-week old SCA1 transgenic mice. Immunohistochemical analysis of cerebellar sections obtained from SCA1 transgenic and littermate control mice confirmed the loss of *Vegfa* expression in Purkinje neurons (Fig. 2C). It is worth noting that *Vegfa* has been validated as a substrate of miR-150 in three previously reported, independent studies (Allantaz et al., 2012; Hua et al., 2006; Ye et al., 2008). These data indicate that a Purkinje cell-specific increase in miR-150 levels occurs concomitantly with a decrease in its targets *Rgs8* and *Vegfa*.

miR-150 can regulate Vegfa expression in mouse N2A neuroblastoma cells

Vegfa has recently become an important therapeutic target in SCA1 (Cvetanovic et al., 2011). We tested whether miR-150 could directly regulate Vegfa expression in the context of a neural-like system. Mouse Neuro2A cells were transiently transfected with varying doses of a synthetic miR-150 miRNA mimic (see Materials and methods) resulting in a 2.5 to 100-fold increase in intracellular miR-150 guide strand levels (not shown). Forty-eight hours post treatment we detected a dose-dependent decrease in the levels of endogenous *Vegfa* mRNA by quantitative PCR (Fig. 3a). In contrast, levels of endogenous mouse *Atxn1*, *Atxn3* or *Htt*, which are not targeted by miR-150, were unaltered at each of the doses tested in N2A cells (not shown). Importantly, western blot analyses confirmed a dose-dependent decrease in endogenous Vegfa expression (Fig. 3b). Vegfa protein levels in N2A cells treated with the miR-150 mimic were nearly 50% less than those

Please cite this article as: Rodriguez-Lebron, E., et al., Altered Purkinje cell miRNA expression and SCA1 pathogenesis, Neurobiol. Dis. (2013), http://dx.doi.org/10.1016/j.nbd.2013.01.019

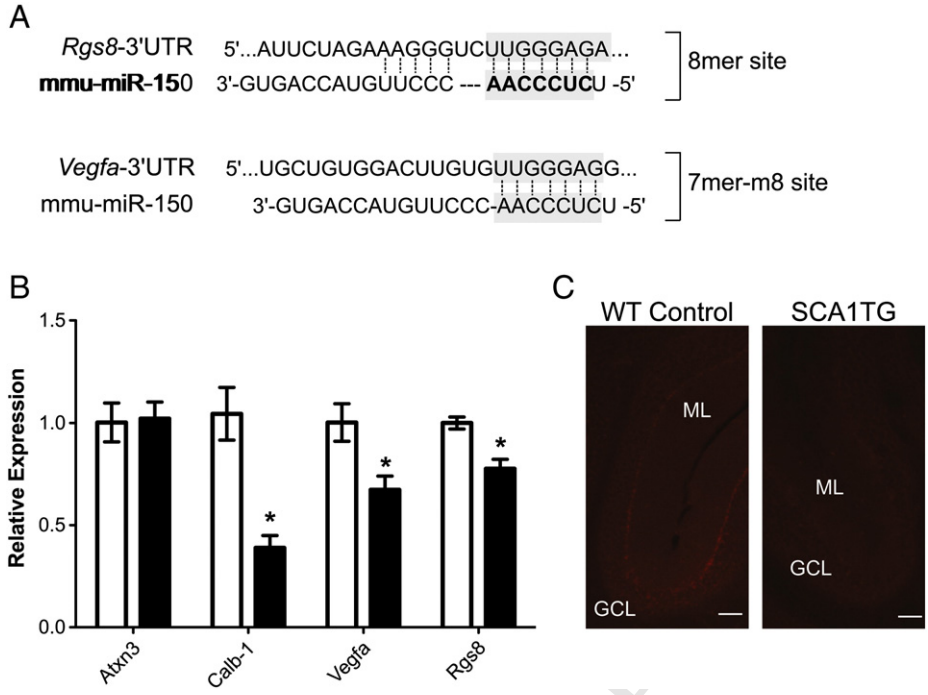

Fig. 2. *Rgs8* and *Vegfa* are targets of miR-150 and are downregulated in SCA1 cerebellum. A) Bioinformatic analysis using publicly available mRNA expression datasets and miRNA target prediction software (TargetScan) identified *Rgs8* and *Vegfa* as two transcripts that are downregulated early in the pathogenesis of SCA1 and are predicted to be targeted by mir-150. B) Quantitative PCR analysis of *Vegfa* and *Rgs8* expression showing a reduction in the levels of both transcripts in adult SCA1 transgenic cerebellum (black bars) compared to littermate controls (white bars). As expected, *Calbindin-1* (Calb-1) expression was also lower in SCA1 transgenic cerebellum while no difference was observed in the levels of *Atxn3*. C) Immunohistochemistry was used to analyze Vegfa1 protein levels in adult SCA1 transgenic mouse brain. Confirming previous reports, SCA1 cerebella (SCA1) had lower levels of Vegfa protein (red signal) when compared to the cerebellum of age-matched littermate controls (WT). Both the molecular (ML) and the granule cell layers (GCL) are identified. Error bars indicate ± std. dev. * = $P<0.05$, student's *t*-test. Bar = 50 μM.

found in N2A cells treated with a control miRNA mimic at the same concentration (Fig. 3b).

To determine if the miR-150 mimic effect was dependent on the presence of a miR-150 binding site sequence in the 3′-UTR of *Vegfa*, we fused the wild-type (Vegfa-3′UTR) or a mutated Vegfa 3′UTR sequence lacking the miR-150 binding site (mut Vegfa-3′UTR) to the 3′end of a luciferase expressing plasmid (Fig. 3c). As expected, transient co-transfections of the miR-150 mimic with the Luciferase-Vegfa-3′UTR expression plasmid led to a dose-dependent reduction in luciferase activity. In contrast, we failed to detect significant changes in luciferase activity following the co-expression of Luciferase-mut Vegfa-3′UTR and the miR-150 mimic. Thus, increased miR-150 activity in N2A cells leads to reduced Vegfa expression and this effect is dependent on the presence of a miR-150 recognition sequence in the 3′UTR of Vegfa.

Suppressing mutant Atxn1 expression partially normalizes the steady-state levels of miR-150 and its target Vegfa in SCA1 transgenic cerebellum

Altered miR-150 levels are observed immediately after the onset of mutant Atxn1 expression in SCA1 transgenic mice (Fig. 1B). If mutant Atxn1 induces these changes, then a reduction in the levels of mutant Atxn1 should be accompanied by normalization (i.e. reduced expression) of miR-150 levels and of its targets (i.e. increased expression). To test this we engineered recombinant adeno-associated vectors (rAAV) expressing anti-Atxn1 (miAtxn1) or control (miCtrl) miRNA mimics under the regulation of a mouse U6 snRNA promoter (Fig. 4A) (Keiser and Davidson, unpublished results). This delivery platform, previously described (Boudreau et al., 2011), also contains an *EGFP* reporter gene downstream of the CMV promoter.

AAV–miAtxn1 and AAV–miCtrl viruses were injected into the deep cerebellar nuclei of 5-week old SCA1 transgenic mice (Fig. 4A). Delivery of AAV virus into the deep cerebellar nuclei results in the transduction of Purkinje neurons via retrograde transport of the virus (Boudreau et al., 2009; Xia et al., 2004). As previously reported, AAV serotype-1 mediates widespread transduction of the mouse Purkinje cell layer (Fig. 4B). Delivery of AAV-miAtxn1 into the cerebellum of 5-week old SCA1 transgenic mice ($n=5$) was associated with varying (from 0.22 to 0.66 fold change) but significant reductions in the levels of mutant Atxn1 transgenic mRNA thirty-five weeks post-injection when compared to AAV–miCtrl or saline injected SCA1 mice (Figs. 4C and D). Notably, AAV–miAtxn1 reduced miR-150 levels (from 0.58 to 0.84 fold change). When analyzing each individual animal for Atxn1 knockdown and miR-150 levels, there was a clear dose dependent correlation. Suppressing mutant Atxn1 expression also induced the recovery of *Calbindin-1* mRNA expression (Figs. 4E and F) in agreement with the therapeutic efficacy of AAV–RNAi against mutant Atxn-1. Finally, *Vegfa* levels were significantly increased (from 1.68 to 2.62 fold change) in AAV–miAtxn1 treated SCA1 transgenic mice, with the extent of increase correlating negatively with miR-150 reduction. Together these results establish a link between the expression of mutant Atxn1 and the levels of miR-150 and its target *Vegfa* in cerebellar Purkinje neurons.

Discussion

Previous studies have established a role for miRNAs in the pathogenesis of polyglutamine diseases (Bilen et al., 2006; Lee et al., 2008; Liu et al., 2012; Packer et al., 2008). Altered miRNA expression was previously observed in SCA1 human brain samples (Persengiev et al., 2011) but the significance of these findings remained largely unexplored. Moreover, investigations into the role that miRNAs play in SCA1 pathogenesis have focused on the deregulation of miRNAs predicted to directly target the 3′UTR of human Atxn1 (Lee et al., 2008; Persengiev et al., 2011). Here, we present the first genome-wide analysis of miRNA expression changes in the cerebellum of SCA1 BO5 mice. In agreement with Persengiev et al. (2011), we find that the expression of mutant Atxn1 leads to modest but significant changes in the steady-state levels of a number of miRNAs. Some of these miRNAs

Please cite this article as: Rodriguez-Lebron, E., et al., Altered Purkinje cell miRNA expression and SCA1 pathogenesis, Neurobiol. Dis. (2013), http://dx.doi.org/10.1016/j.nbd.2013.01.019

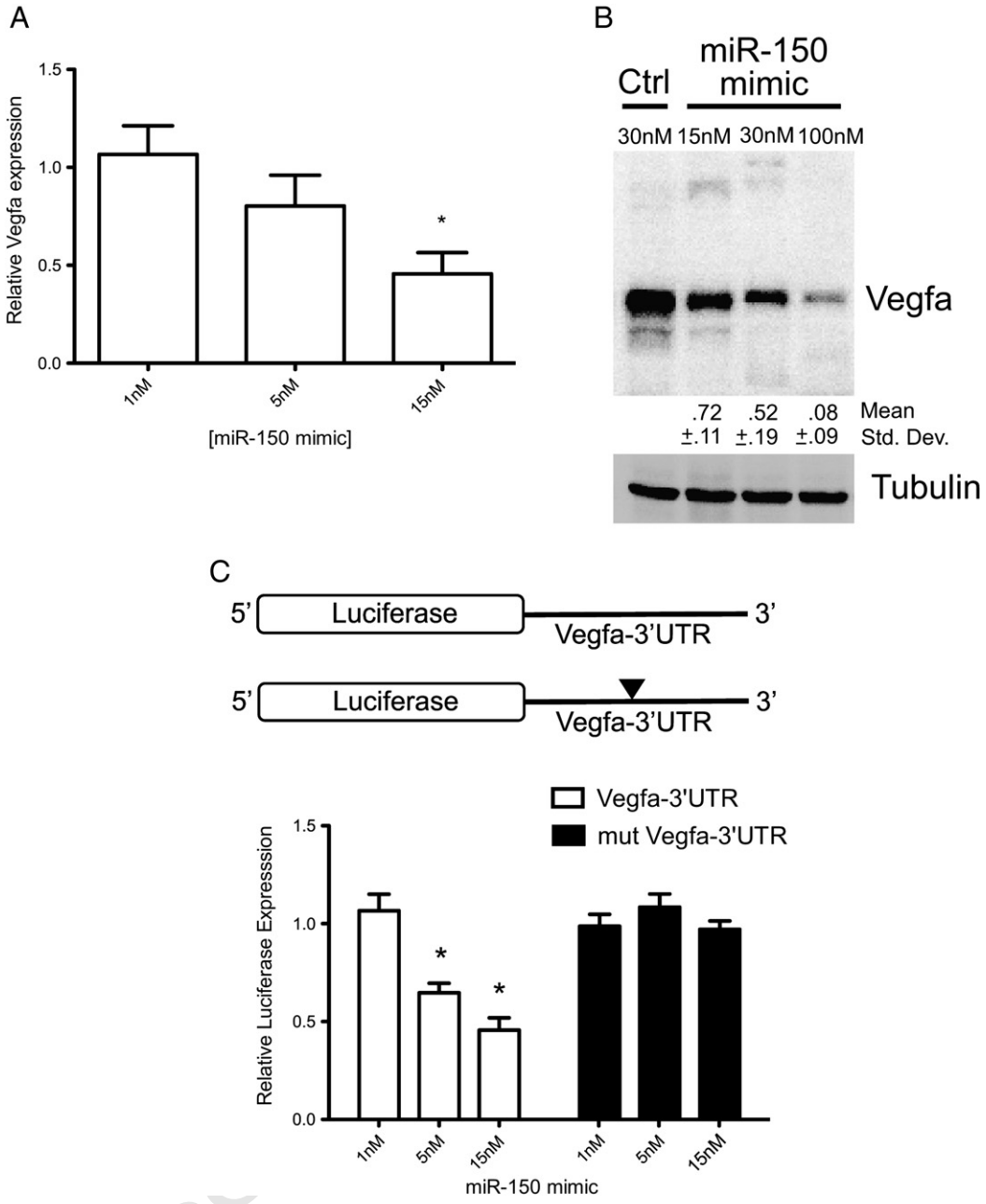

Fig. 3. MiR-150 mediates post-transcriptional gene silencing of *Vegfa* through a conserved binding site sequence in the 3′UTR of the *Vegfa* transcript. A) Neuro2a cells were treated with three different doses (1 nM, 5 nM and 15 nM) of a chemically modified miR-150 miRNA mimic (*MiRVana*™ miRNA mimics). Quantitative PCR analysis revealed a dose-dependent reduction in *Vegfa* transcript levels 48-h post-treatment (5 nM: 20% and 15 nM: 54%). B) MiR-150-mediated the reduction of *Vegfa* transcript levels coincided with a dose-dependent reduction in Vegfa protein levels as shown by western blot analysis 48-h post treatment. Mean expression levels of Vegfa, plus or minus the standard deviation (numbers below the anti-Vegfa western blot), were calculated using data obtained from three independent experiments (see Materials and methods). C) The 3′UTR of Vegfa, including the conserved miR-150 target site sequence, was cloned downstream of a *Renilla* luciferase expression plasmid. A second construct carried the same 3′UTR Vegfa sequence with a mutated miR-150 binding site. Following transient co-transfection, luciferase activity assays revealed that the miR-150 mimic could interfere with the expression of *Renilla* luciferase in a dose-dependent manner when fused to the wild-type (white bars) but not the mutant Vegfa-3′UTR sequence (black bars). * = significance at $P<0.05$. Error bars in A and C indicate std. dev.

are known to play critical roles in neuronal development and function and modest but chronic changes in their steady-state levels are likely to influence disease progression and severity. Importantly, the steady-state levels of several miRNAs were altered prior to phenotypic onset in SCA1 transgenic mice implicating them in the genesis of disease. Finally, we provide evidence that an increase in miR-150 levels is likely to influence SCA1 pathogenesis by suppressing the expression of *Rgs8*, and contributing to the reduction of *Vegfa* in cerebellar Purkinje neurons.

Perinatal expression of mutant Atxn1 is required for full disease manifestation in SCA1 transgenic mice (Barnes et al., 2011; Serra et al., 2006) suggesting a link between mutant Atxn1 pathogenicity and post-natal cerebellar development. We find alterations in the expression of several miRNAs in the cerebellum of SCA1 transgenic mice during this critical period. In particular, miR-335 expression was significantly upregulated at this time point. Intriguingly, climbing fiber activation of Purkinje cells, which is abnormal in SCA1 transgenic mice, normally modulates miR-335 levels in Purkinje cells (Barmack et al., 2010; Barnes et al., 2011). It is possible that altered miR-335 expression drives mutant Atxn1 pathogenicity during post-natal development by altering climbing fiber-Purkinje cell physiology. It could accomplish this, for example, by deregulating the expression of its targets

Please cite this article as: Rodriguez-Lebron, E., et al., Altered Purkinje cell miRNA expression and SCA1 pathogenesis, Neurobiol. Dis. (2013), http://dx.doi.org/10.1016/j.nbd.2013.01.019

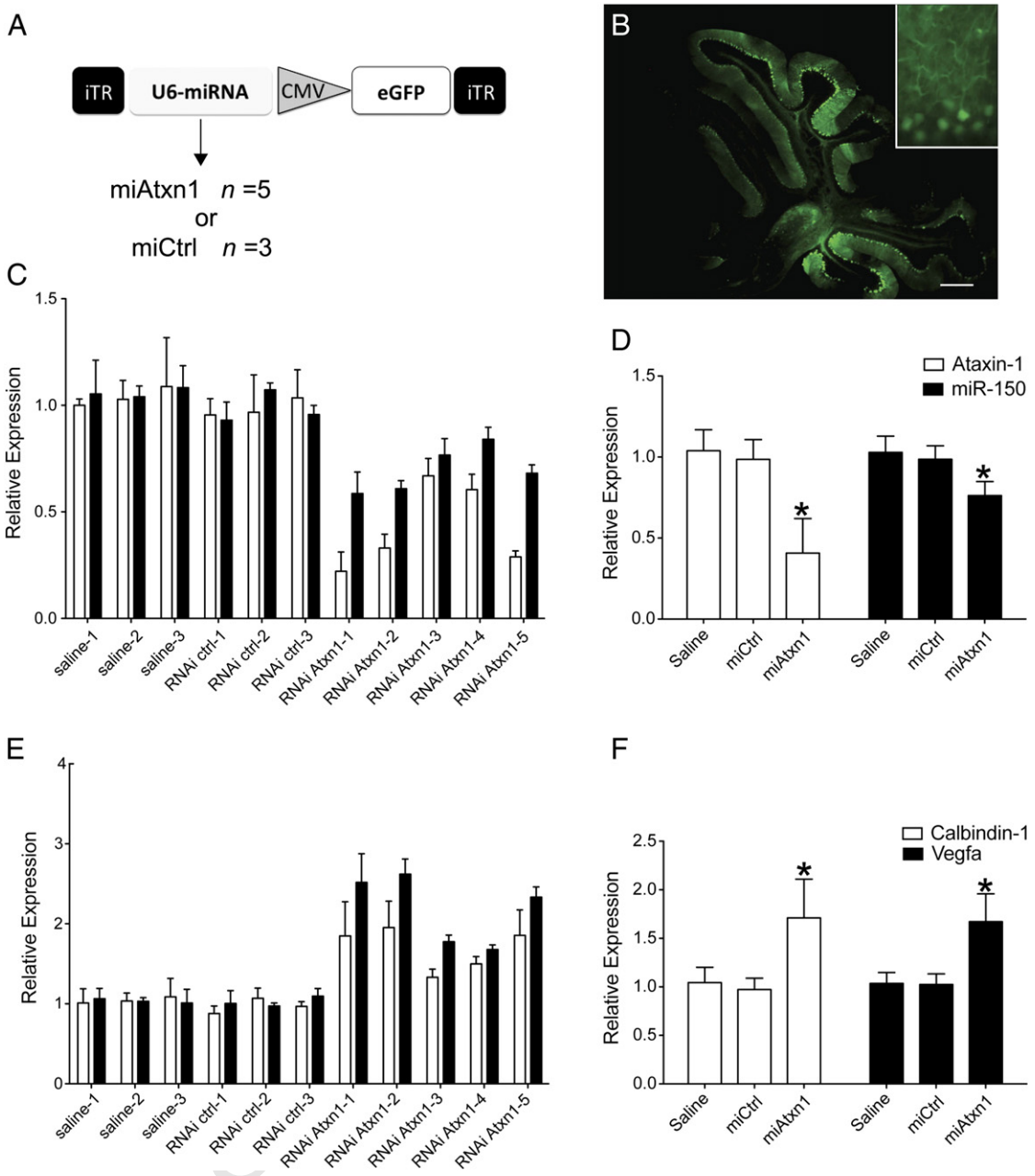

Fig. 4. Silencing mutant Ataxin-1 expression partially normalizes endogenous miR-150 and *Vegfa* transcript levels in SCA1 transgenic mouse cerebellum. A) Control (miCtrl) or mutant Ataxin-1-targeting (miAtxn1) artificial miRNAs were cloned into a recombinant adeno-associated expression vector (rAAV) under the regulation of a mouse U6 snRNA promoter. The green fluorescent protein (GFP) coding sequence was placed downstream of the RNAi expression cassette under the regulation of the *Cytomegalovirus* (CMV)-derived immediate-early promoter. B) A total of 11, 5-week old SCA1 transgenic mice received intracerebellar injections of either rAAV encoding miCtrl (RNAi ctrl, $n=3$), miAtxn1 (RNAi Atxn1, $n=5$) or saline (saline, $n=3$). Thirty-five weeks post-delivery, there was widespread GFP expression throughout the Purkinje cell layer of AAV-injected SCA1 transgenic mice. Shown is a representative section from SCA1 transgenic mice expressing rAAV–miAtxn1 virus. The inset on the top right corner illustrates the pattern of GFP expression throughout the Purkinje cell soma and dendrites. C) Quantitative PCR analysis of transgenic mutant *Atxn1* mRNA (white bars) and *mmu-miR-150* (black bars) expression in SCA1 transgenic mice receiving a saline injection (saline-1, -2 and -3), rAAV–miCtrl injections (RNAi ctrl-1, -2 and -3) and rAAV–miAtxn1 injections (RNAi Atxn1-1, -2, -3, -4 and -5). A strong reduction in mutant *Atxn1* levels led to a mutant *Atxn1* dose-dependent partial normalization of miR-150 levels (i.e. reduced levels compared to control injected SCA1 mice) in SCA1 transgenic mice expressing the anti-mutant Atxn1 miRNA. D) Per group analysis of the data presented in C. E) Quantitative PCR analysis of *Calbindin-1* (white bars) and *Vegfa* (black bars) expression in the cerebellum of the same rAAV-treated SCA1 transgenic mice. A dose dependent, partial normalization of *Calbindin-1* and *Vegfa* was observed in SCA1 transgenic mice that displayed reduced levels of mutant *Atxn1* and miR-150 in C. Error bars in C and E = ± std. dev of technical replicates. Error bars in D and F = ± SEM. * = $P<0.05$, student's *t*-test.

Calbindin-1 and *14-3-3θ* in Purkinje neurons (Barmack et al., 2010; Qian et al., 2012) during this critical post-natal period. Alternatively, changes in miR-335 expression might ensue as a consequence of altered climbing fiber-Purkinje cell physiology during the early stages of disease. Regardless, our results support a functional role for miR-335 in the post-natal physiological deficiencies observed in SCA1 transgenic mouse cerebellum.

Loss of *Vegfa* expression in SCA1 Purkinje neurons contributes to disease pathogenesis (Cvetanovic et al., 2011). Cvetanovic et al. (2011) showed that mutant and wild-type Atxn1 can directly occupy the *Vegfa* promoter and repress its transcriptional activity. Here, we present evidence for an additional layer of mutant Atxn1-mediated misregulation of *Vegfa* expression in SCA1 Purkinje neurons. Our data, together with the findings of Cvetanovic et al., support a model in

Please cite this article as: Rodriguez-Lebron, E., et al., Altered Purkinje cell miRNA expression and SCA1 pathogenesis, Neurobiol. Dis. (2013), http://dx.doi.org/10.1016/j.nbd.2013.01.019

which mutant Atxn1 can directly repress transcriptional activity at the *Vegfa* promoter and also inhibiting *Vegfa* gene expression at the post-transcriptional level via miR-150 induction (Fig. 5). Our data further validates *Vegfa* as a miR-150 target (Allantaz et al., 2012; Hua et al., 2006; Ye et al., 2008), however, the mechanism(s) by which mutant Atxn1 induces an increase in miR-150 steady-state levels remains undetermined. One possibility is that a reduction in Atxn1's transcriptional repressive activity in SCA1 de-represses activity at miRNA promoters, including miR-150. Alternatively, miR-150 levels could increase in response to an unknown gain of toxic function in mutant Atxn1. Ongoing experiments aim to address these interesting questions.

RNAi-mediated suppression of mutant Atxn-1 remains a highly promising therapeutic approach to SCA1. Reducing mutant Atxn-1 expression in Purkinje cells of SCA1 transgenic mice led to significant normalization of several disease markers, including *Calbindin-1* and *Vegfa*. The recovery in Vegfa levels is likely the consequence of both reduced promoter occupancy by mutant Atxn-1 and reduced miR-150 activity. These results highlight an important aspect of RNAi-based therapy for SCA1 and other polyglutamine diseases: reducing the expression of the mutant protein can lead to a normalization of neuronal cell function in numerous fronts.

In summary, we provide evidence for changes in miRNA expression in pre- and post-symptomatic SCA1 transgenic mice cerebella. Furthermore, we provide examples of how altered miRNA expression may promote SCA1 pathogenesis, thus, shedding light into new areas of disease pathogenesis. Using an RNAi-based approach, we also demonstrate the potential use of miRNA profiling as a surrogate marker of disease. Further dissecting the individual contributions of altered miRNA expression to disease pathogenesis may reveal new molecular targets for therapeutic development.

Acknowledgments

The authors thank Eric Kaiser and Ines Martins for the technical assistance and Dr. A Madan for the assistance with miRNA microarray analysis. This work was supported in part by the NIH grants NS 44093, NS 50210 (to B.L.D), and NS 072229 (to E.R.L) and the National Ataxia Foundation Fellowship (G.L).

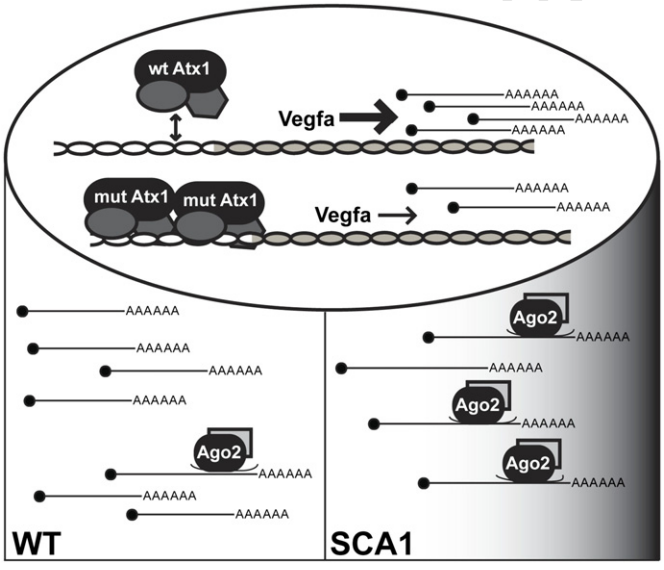

Fig. 5. Possible mechanisms underlying reduced Vegfa expression in SCA1 Purkinje cells. Nucleus: Mutant Ataxin-1, together with DNA binding proteins, can occupy the Vegfa promoter and repress transcriptional activity (Cvetanovic et al., 2011). It is unclear if wild type Ataxin-1 similarly regulates Vegfa transcription. Cytosol: Vegfa expression is also under the post-transcriptional regulation of miRNAs (WT box). However, increased miR-150 activity in SCA1 Purkinje cells (SCA1 gradient box) can act to further suppress Vegfa expression via post-transcriptional gene silencing.

References

Allantaz, F., et al., 2012. Expression profiling of human immune cell subsets identifies miRNA–mRNA regulatory relationships correlated with cell type specific expression. PLoS One 7, e29979.
Banfi, S., et al., 1994. Identification and characterization of the gene causing type 1 spinocerebellar ataxia. Nat. Genet. 7, 513–520.
Barmack, N.H., et al., 2010. Climbing fibers induce microRNA transcription in cerebellar Purkinje cells. Neuroscience 171, 655–665.
Barnes, J.A., et al., 2011. Abnormalities in the climbing fiber-Purkinje cell circuitry contribute to neuronal dysfunction in ATXN1[82Q] mice. J. Neurosci. 31, 12778–12789.
Bilen, J., et al., 2006. MicroRNA pathways modulate polyglutamine-induced neurodegeneration. Mol. Cell. 24, 157–163.
Boudreau, R.L., et al., 2009. Artificial microRNAs as siRNA shuttles: improved safety as compared to shRNAs in vitro and in vivo. Mol. Ther. 17, 169–175.
Boudreau, R.L., et al., 2011. Rational design of therapeutic siRNAs: minimizing off-targeting potential to improve the safety of RNAi therapy for Huntington's disease. Mol. Ther. 19, 2169–2177.
Burright, E.N., et al., 1995. SCA1 transgenic mice: a model for neurodegeneration caused by an expanded CAG trinucleotide repeat. Cell 82, 937–948.
Crespo-Barreto, J., et al., 2010. Partial loss of ataxin-1 function contributes to transcriptional dysregulation in spinocerebellar ataxia type 1 pathogenesis. PLoS Genet. 6, e1001021.
Cvetanovic, M., et al., 2011. Vascular endothelial growth factor ameliorates the ataxic phenotype in a mouse model of spinocerebellar ataxia type 1. Nat. Med. 17, 1445–1447.
Durr, A., 2010. Autosomal dominant cerebellar ataxias: polyglutamine expansions and beyond. Lancet Neurol. 9, 885–894.
Fernandez-Funez, P., et al., 2000. Identification of genes that modify ataxin-1-induced neurodegeneration. Nature 408, 101–106.
Friedman, R.C., et al., 2009. Most mammalian mRNAs are conserved targets of microRNAs. Genome Res. 19, 92–105.
Gatchel, J.R., et al., 2008. The insulin-like growth factor pathway is altered in spinocerebellar ataxia type 1 and type 7. Proc. Natl. Acad. Sci. U. S. A. 105, 1291–1296.
Grimson, A., et al., 2007. MicroRNA targeting specificity in mammals: determinants beyond seed pairing. Mol. Cell. 27, 91–105.
Hua, Z., et al., 2006. MiRNA-directed regulation of VEGF and other angiogenic factors under hypoxia. PLoS One 1, e116.
Kim, V.N., et al., 2009. Biogenesis of small RNAs in animals. Nat. Rev. Mol. Cell Biol. 10, 126–139.
Lam, Y.C., et al., 2006. ATAXIN-1 interacts with the repressor Capicua in its native complex to cause SCA1 neuropathology. Cell 127, 1335–1347.
Lee, Y., et al., 2008. miR-19, miR-101 and miR-130 co-regulate ATXN1 levels to potentially modulate SCA1 pathogenesis. Nat. Neurosci. 11, 1137–1139.
Lewis, B.P., et al., 2005. Conserved seed pairing, often flanked by adenosines, indicates that thousands of human genes are microRNA targets. Cell 120, 15–20.
Lim, J., et al., 2008. Opposing effects of polyglutamine expansion on native protein complexes contribute to SCA1. Nature 452, 713–718.
Lin, X., et al., 2000. Polyglutamine expansion down-regulates specific neuronal genes before pathologic changes in SCA1. Nat. Neurosci. 3, 157–163.
Liu, N., et al., 2012. The microRNA miR-34 modulates ageing and neurodegeneration in *Drosophila*. Nature 482, 519–523.
Matilla-Duenas, A., et al., 2010. Cellular and molecular pathways triggering neurodegeneration in the spinocerebellar ataxias. Cerebellum 9, 148–166.
Orr, H.T., 2012. Cell biology of spinocerebellar ataxia. J. Cell Biol. 197, 167–177.
Orr, H.T., Zoghbi, H.Y., 2007. Trinucleotide repeat disorders. Annu. Rev. Neurosci. 30, 575–621.
Packer, A.N., et al., 2008. The bifunctional microRNA miR-9/miR-9* regulates REST and CoREST and is downregulated in Huntington's disease. J. Neurosci. 28, 14341–14346.
Persengiev, S., et al., 2011. Genome-wide analysis of miRNA expression reveals a potential role for miR-144 in brain aging and spinocerebellar ataxia pathogenesis. Neurobiol. Aging 32 (2316), e17–e27.
Qian, Z., et al., 2012. Climbing fiber activity reduces 14-3-3-theta regulated GABA(A) receptor phosphorylation in cerebellar Purkinje cells. Neuroscience 201, 34–45.
Schaefer, A., et al., 2007. Cerebellar neurodegeneration in the absence of microRNAs. J. Exp. Med. 204, 1553–1558.
Seidel, K., et al., 2012. Brain pathology of spinocerebellar ataxias. Acta Neuropathol. 124, 1–21.
Serra, H.G., et al., 2004. Gene profiling links SCA1 pathophysiology to glutamate signaling in Purkinje cells of transgenic mice. Hum. Mol. Genet. 13, 2535–2543.
Serra, H.G., et al., 2006. RORalpha-mediated Purkinje cell development determines disease severity in adult SCA1 mice. Cell 127, 697–708.
Takahashi, T., et al., 2010. Polyglutamine diseases: where does toxicity come from? What is toxicity? Where are we going? J. Mol. Cell Biol. 2, 180–191.
Tsou, W.L., et al., 2011. Splice isoform-specific suppression of the Cav2.1 variant underlying spinocerebellar ataxia type 6. Neurobiol. Dis. 43, 533–542.
Verbeek, D.S., van de Warrenburg, B.P., 2011. Genetics of the dominant ataxias. Semin. Neurol. 31, 461–469.
Xia, H., et al., 2004. RNAi suppresses polyglutamine-induced neurodegeneration in a model of spinocerebellar ataxia. Nat. Med. 10, 816–820.
Ye, W., et al., 2008. The effect of central loops in miRNA:MRE duplexes on the efficiency of miRNA-mediated gene regulation. PLoS One 3, e1719.
Zoghbi, H.Y., Orr, H.T., 2009. Pathogenic mechanisms of a polyglutamine-mediated neurodegenerative disease, spinocerebellar ataxia type 1. J. Biol. Chem. 284, 7425–7429.